A Fourth-Order Runge–Kutta in the Interaction Picture Method for Simulating Supercontinuum Generation in Optical Fibers

Johan Hult

Abstract—An efficient algorithm, which exhibits a fourth-order global accuracy, for the numerical solution of the normal and generalized nonlinear Schrödinger equations is presented. It has applications for studies of nonlinear pulse propagation and spectral broadening in optical fibers. Simulation of supercontinuum generation processes, in particular, places high demands on numerical accuracy, which makes efficient high-order schemes attractive. The algorithm that is presented here is an adaptation for use in the nonlinear optics field of the fourth-order Runge–Kutta in the Interaction Picture (RK4IP) method, which was originally developed for studies on Bose–Einstein condensates. The performance of the RK4IP method is validated and compared to a number of conventional methods by modeling both the propagation of a second-order soliton and the generation of supercontinuum radiation. It exhibits the expected global fourth-order accuracy for both problems studied and is the most accurate and efficient of the methods tested.

Index Terms—Nonlinear optics, nonlinear Schrödinger equation (NLSE), numerical analysis, optical solitons, Runge–Kutta method, split-step Fourier method, supercontinuum radiation.

I. INTRODUCTION

EXTREME spectral broadening can be achieved in a variety of nonlinear media using intense narrowband optical pulses, yielding broadband spectrally continuous radiation which is known as a supercontinuum. Broadband supercontinuum light sources have found applications in fields such as spectroscopy, microscopy, pulse compression, telecommunications, and optical device testing [1], [2]. Of particular interest to practical applications is the high efficiency of supercontinuum generation in optical fibers. Normally, a photonic crystal fiber (PCF) [3] or a highly nonlinear fiber (HNLF) [4] has been employed for this purpose, but supercontinuum generation in a conventional fiber is also possible [5].

A nonlinear Schrödinger equation (NLSE) can be used to study pulse propagation in optical fibers and has extensively been used for modeling of optical-fiber communications systems and for the study of optical solitons. In its standard form,

however, it only describes the effects of second-order dispersion and self-phase modulation (SPM). To accurately describe the process of supercontinuum generation, addition of terms representing loss, higher order dispersion, stimulated Raman scattering, and frequency dependence of the nonlinear response is necessary, resulting in a generalized NLSE (GNLSE) [6]. The NLSE and GNLSE are nonlinear partial differential equations (PDEs) that, in almost all cases, cannot analytically be solved. A numerical approach is therefore necessary. Numerical modeling of supercontinuum generation can help in shedding light on the underlying spectral broadening processes [2]. It can also be used to guide fiber design and pump laser choice in order to achieve particular desired properties of the supercontinuum radiation [7]. Numerical solutions of the GNLSE are often time-consuming, in particular, for long pump pulses or very broad spectra, so efficient numerical integration schemes are desirable.

The most commonly employed numerical scheme for solving the GNLSE is the split-step Fourier method [6]. In the split-step method, dispersive and nonlinear effects are separately integrated, and the results are combined to construct the full solution. The dispersive term, which is linear, is evaluated in the frequency domain through the use of the fast Fourier transform (FFT), whereas the nonlinear term is treated in the time domain. Simple split-step schemes of global second- [8] or third-order [9]–[11] accuracy are normally employed. It is also possible to construct higher order split-step schemes such as the fourth-order scheme of Blow and Wood [12]. However, global accuracy cannot exceed the accuracy of the method that is used to integrate the nonlinear step, and for this purpose, Runge–Kutta or implicit schemes are normally used.

The Gross–Pitaevskii equation is a nonlinear PDE that is used to describe the dynamics of Bose–Einstein condensates. It has a structure that is similar to the optical NLSE and GNLSE equations, but with time and space variables playing opposite roles. A highly efficient and accurate algorithm, which is called the fourth-order Runge–Kutta in the interaction picture (RK4IP) method and is described in detail by Caradoc-Davies [13], has been developed to solve the Gross–Pitaevskii equation. This RK4IP method has successfully been employed for numerical studies of a range of phenomena in Bose–Einstein condensates [14]–[16].

The RK4IP method is closely related to the split-step Fourier method. The algorithm is based on transforming the problem into an interaction picture, which allows the use of conventional

The author is with the Department of Chemical Engineering, University of Cambridge, CB2 3RA Cambridge, U.K. (e-mail: jfh36@cam.ac.uk).

explicit techniques to step the solution forward. A high efficiency is achieved by combining a fourth-order Runge–Kutta technique for stepping, with an appropriate choice of separation between the normal and interaction pictures. The resulting method exhibits fourth-order global accuracy, is memory efficient, and is easy to implement in solving the NLSE or GNLSE equations in optical fibers.

This paper is organized as follows. First, the NLSE and GNLSE equations are introduced; then, a short review of the split-step Fourier method and its different implementations is given. The RK4IP algorithm and its implementation for the study of optical-pulse propagation are then described. Next, the performance of the RK4IP method is validated and compared to a number of split-step Fourier schemes for two different nonlinear optical-pulse-propagation problems. The propagation of a second-order soliton, as well as the generation of broadband supercontinuum radiation, is studied. The results of these comparisons are discussed, and finally, the conclusion follows.

II. NUMERICAL METHOD

A. Nonlinear Schrödinger Equation (NLSE)

The NLSE, which can be written as

$$\frac{\partial A}{\partial z} = -i\frac{\beta_2}{2}\frac{\partial^2 A}{\partial T^2} + i\gamma|A|^2 A \tag{1}$$

governs the propagation of light in a lossless optical fiber exhibiting second-order dispersion [6]. In (1), $A(z,t)$ is the complex field envelope, z is the distance, t is the retarded time traveling at the envelope group velocity, β_2 is the second-order dispersion, and γ is the nonlinear coefficient. The first term on the right-hand side is a linear term describing dispersion, whereas the second term is nonlinear and describes SPM. In the anomalous dispersion regime, where $\beta_2 < 0$, self-preserving soliton solutions to (1) exist [17].

B. GNLSE

Various forms of the GNLSE can be obtained from the NLSE (1) by including terms describing the effects of fiber loss, higher order dispersion, stimulated Raman scattering, and frequency dependence of the nonlinear response [12], [18]. GNLSE equations can be derived from analytical simplifications of Maxwell's equations [6]. A form of the GNLSE that is commonly employed for numerical simulations of supercontinuum generation is [19]

$$\frac{\partial A}{\partial z} = -\frac{\alpha}{2}A - \left(\sum_{k\geq 2}\beta_n\frac{i^{n-1}}{n!}\frac{\partial^n}{\partial T^n}\right)A + i\gamma\left(1+\frac{1}{\omega_0}\frac{\partial}{\partial T}\right)$$
$$\times\left((1-f_R)A|A|^2 + f_R A\int_0^\infty h_R(\tau)\,|A(z,T-\tau)|^2\,d\tau\right) \tag{2}$$

where α is the attenuation constant, and β_n are the higher order dispersion coefficients obtained by a Taylor series expansion of

the propagation constant $\beta(\omega)$ around the center frequency ω_0. The fractional contribution of the delayed Raman response to nonlinear polarization is represented by f_R, in which a value of $f_R = 0.18$ is often assumed [20]. In (2), $h_R(t)$ is the Raman response function of a silica fiber, in which the analytical form proposed by Hollenbeck and Cantrell [21] was used in this paper. The first and second terms on the right-hand side of (2) describe fiber loss and dispersion, respectively. The third term describes the nonlinear effects. The temporal derivative in this term is responsible for self-steepening and optical shock formation, whereas the convolution integral describes the delayed Raman response, which leads to effects such as intrapulse Raman scattering.

C. Review of the Split-Step Fourier Method

For numerical integration, it is useful to represent (1) and (2) in the form

$$\frac{\partial A}{\partial z} = (\hat{D} + \hat{N})A \tag{3}$$

where $\hat{D}$ is a dispersion operator, and $\hat{N}$ is a nonlinear operator. For the NLSE (1), they are given by

$$\hat{D} = -i\frac{\beta_2}{2}\frac{\partial^2}{\partial T^2} \tag{4}$$

$$\hat{N} = i\gamma|A|^2 \tag{5}$$

whereas for the GNLSE (2), they are given by

$$\hat{D} = -\frac{\alpha}{2} - \left(\sum_{k\geq 2}\beta_n\frac{i^{n-1}}{n!}\frac{\partial^n}{\partial T^n}\right) \tag{6}$$

$$\hat{N} = i\gamma\frac{1}{A}\left(1+\frac{1}{\omega_0}\frac{\partial}{\partial T}\right)$$
$$\times\left((1-f_R)A|A|^2 + f_R A\int_0^\infty h_R(\tau)\,|A(z,T-\tau)|^2\,d\tau\right). \tag{7}$$

In the symmetric split-step Fourier method, the solution to (3) over a step h is approximated by

$$A(z+h,T) = \exp\left(\frac{h}{2}\hat{D}\right)\exp\left(\int_z^{z+h}\hat{N}(z')dz'\right)$$
$$\times\exp\left(\frac{h}{2}\hat{D}\right)A(z,T) \tag{8}$$

where the exponential dispersion operator is conveniently evaluated in the Fourier domain through the use of the FFT. Since the dispersion and nonlinear operators do not commute, in general, the solution (8) is only an approximation to the exact solution, with a global error that is second-order in the step size $O(h^2)$. Many different approaches in approximating the nonlinear term, which are described by the integral in the middle exponential, have been reported. The simplest consists of approximating it with $\exp(h\hat{N})$, which will henceforward

be referred to as the symmetric split-step method [8]. Second- and fourth-order Runge–Kutta methods (symmetric split-step RK2 and symmetric split-step RK4, respectively) [9]–[11], as well as an implicit scheme (symmetric split-step Agrawal) [6], have also been employed.

Simpler schemes are the split-step and reduced split-step methods [8], which rely on approximating (3) with $A(z + h, T) = \exp(h\hat{D})\exp(h\hat{N})A(z, T)$, leading to a global error that is only first order in the step size $O(h)$. It is also possible to construct higher order split-step schemes by various forms of extrapolation [8], [12], [22]. One popular scheme is the one introduced by Blow and Wood [12], in which four forward steps of length h are taken, followed by one backward step of length $2h$, and then four more forward steps of length h, which leads to a globally fourth-order accurate scheme $O(h^4)$. Implementations of this scheme with propagation using the simple split-step, symmetric split-step RK2, and symmetric split-step RK4 methods, respectively, will here be referred to as the Blow–Wood SS, Blow–Wood RK2, and Blow–Wood RK4 methods. It should be noted that none of the aforementioned Fourier split-step schemes can posses a global accuracy exceeding that of the numerical scheme used to integrate the nonlinear term, as will be apparent later on.

D. Fourth-Order Runge–Kutta in the Interaction Picture Method

In the RK4IP method, the NLSE is transformed into an interaction picture in order to separate the effect of dispersion contained in $\hat{D}$ from the nondispersive terms in $\hat{N}$. This allows the use of explicit techniques to put the solution forward. Field envelope A is transformed into the interaction picture representation A_I by

$$A_I = \exp\left(-(z - z')\hat{D}\right) A \qquad (9)$$

where z' is the separation distance between the interaction and normal pictures. Differentiating (9) gives the evolution of A_I

$$\frac{\partial A_I}{\partial z} = \hat{N}_I A_I \qquad (10)$$

where

$$\hat{N}_I = \exp\left(-(z - z')\hat{D}\right) \hat{N} \exp\left((z - z')\hat{D}\right) \qquad (11)$$

is the nonlinear operator in the interaction picture. The differential equation (10) can now be solved by using conventional explicit schemes such as Runge–Kutta methods, as the stiff linear parts of the PDE (3) have now been ameliorated by moving into the interaction picture.

A straightforward solution of (10), which employs a fourth-order Runge–Kutta method, with the exponential operators evaluated in the frequency domain, would require 16 FFTs per step. The use of the RK4IP algorithm, however, reduces by half the required number of FFTs [13]. This is achieved by choosing the step midpoint as the separation distance $z' = z + h/2$, which eliminates the dispersion exponentials in (11) for the two midpoint trajectories k_2 (12c) and k_3 (12d). The algorithm that

advances $A(z, T)$ to $A(z + h, T)$ in a spatial step h, expressed in the normal picture A, is now written as

$$A_I = \exp\left(\frac{h}{2}\hat{D}\right) A(z, T) \qquad (12a)$$

$$k_1 = \exp\left(\frac{h}{2}\hat{D}\right) \left[h\hat{N}(A(z, T))\right] A(z, T) \qquad (12b)$$

$$k_2 = h\hat{N}(A_I + k_1/2)[A_I + k_1/2] \qquad (12c)$$

$$k_3 = h\hat{N}(A_I + k_2/2)[A_I + k_2/2] \qquad (12d)$$

$$k_4 = h\hat{N}\left(\exp\left(\frac{h}{2}\hat{D}\right)(A_I + k_3)\right)$$
$$\times \exp\left(\frac{h}{2}\hat{D}\right)[A_I + k_3] \qquad (12e)$$

$$A(z+h, T) = \exp\left(\frac{h}{2}\hat{D}\right)[A_I + k_1/6 + k_2/3 + k_3/3] + k_4/6. \qquad (12f)$$

The transformation into the normal picture (12f) introduces an overhead of two FFTs per step; however, this overhead is eliminated by keeping the last trajectory k_4 (12e) in the normal picture. In total, each step thus requires four evaluations of the nonlinear operator $\hat{N}$ and four evaluations of the exponential dispersion operator $\exp(h\hat{D}/2)$, which requires eight FFTs. The RK4IP algorithm has a local error which is a fifth-order $O(h^5)$ and, thus, is a globally fourth-order accurate method $O(h^4)$.

It should be noted that, in principle, higher order Runge–Kutta schemes could be implemented in the same fashion; however, the advantageous position of the midpoints is lost for higher order schemes, thus hindering any further increases in computational efficiency.

III. NUMERICAL RESULTS

A. Second-Order Soliton

The performance of the suggested RK4IP numerical scheme was first tested by considering the propagation of a second-order soliton using the NLSE (1). Analytical solutions exist for the periodic evolution of such higher order solitons [6], which constitute ideal test cases. An anomalous fiber with $\beta_2 = -0.01 \text{ ps}^2 \cdot \text{m}^{-1}$ and $\gamma = 0.01 \text{ W}^{-1} \cdot \text{m}^{-1}$ was employed to study soliton propagation. The initial pulse corresponding to a second-order soliton with an intensity full-width at half-maximum (FWHM) pulselength of $T_{\text{FWHM}} = 100$ fs under these conditions was $A(0, T) = \sqrt{P_0}\text{sech}(T/T_0)$, where the peak power $P_0 = 2^2|\beta_2|/\gamma T_0^2 = 1.24$ kW, and the width $T_0 = T_{\text{FWHM}}/2\ln(1 + \sqrt{2}) = 56.7$ fs. The corresponding soliton period was 0.506 m, and the field envelope A was discretized into $N = 2^{12}$ temporal gridpoints.

In order to compare the performance of different numerical schemes, the average relative intensity error ε, which is defined by

$$\varepsilon = \frac{\sum_{k=1}^{N} \left||A_k^{\text{comp}}|^2 - |A_k^{\text{true}}|^2\right| / N}{\max\left(|A^{\text{true}}|^2\right)} \qquad (13)$$

after one soliton period was used. In (13), N is the number of temporal grid points, A_k^{true} is the analytical expression for the
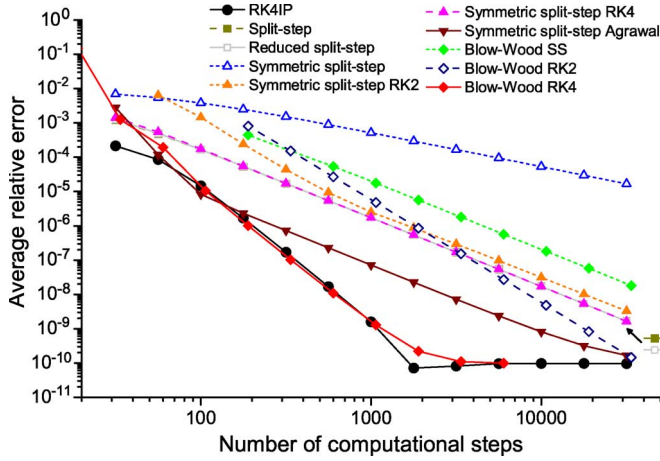
Fig. 1. Average relative error versus the number of computational steps for the propagation of a second-order soliton over one soliton period.

TABLE I
FIBER PARAMETERS FOR PCF USED IN THE SIMULATION OF SUPERCONTINUUM GENERATION

β_2	$-1.276 \times 10^{-2} \mathrm{ps}^2 \cdot \mathrm{m}^{-1}$
β_3	$8.119 \times 10^{-5} \mathrm{ps}^3 \cdot \mathrm{m}^{-1}$
β_4	$-1.321 \times 10^{-7} \mathrm{ps}^4 \cdot \mathrm{m}^{-1}$
β_5	$3.032 \times 10^{-10} \mathrm{ps}^5 \cdot \mathrm{m}^{-1}$
β_6	$-4.196 \times 10^{-13} \mathrm{ps}^6 \cdot \mathrm{m}^{-1}$
β_7	$2.570 \times 10^{-16} \mathrm{ps}^7 \cdot \mathrm{m}^{-1}$
γ	$0.045 \mathrm{W}^{-1} \mathrm{m}^{-1}$
L	0.1 m

field envelope of the second-order soliton at grid point k, and A_k^{comp} is the calculated result at the same grid point.

The error ε for the RK4IP method as a function of the number of computational steps N_{steps} employed is shown in Fig. 1, with a logarithmic scale on both axes. The errors obtained using the split-step methods listed in Section II-C are also shown for comparison.

The most accurate methods are the RK4IP and Blow–Wood RK4 methods, which both exhibit an asymptotic slope of -4 and, thus, a global fourth-order accuracy, until the machine accuracy is reached at $\varepsilon \approx 10^{-10}$. The two other implementations of the Blow–Wood scheme are seen to perform much worse, with a third-order accuracy for the Blow–Wood RK2 method and a second-order accuracy for the Blow–Wood SS method. In these two cases, the theoretical accuracy of the operator-splitting scheme is not realized as they are limited by the accuracy of the schemes that are used to integrate the nonlinear terms. Of all the symmetric split-step methods, the best performance is achieved using the implicit symmetric split-step Agrawal method, which asymptotically exhibits a second-order accuracy just like the symmetric split-step RK2 and symmetric split-step RK4 methods, but with a higher accuracy for large step sizes. The symmetric split-step method, which uses the crudest approximation of the nonlinear term, on the other hand, only achieves first-order accuracy. A curiosity is that both the simple split-step methods achieve second-order accuracy for the case of the simple nonlinearity $i\gamma|A|^2$ of the NLSE (1), whereas in the general case, they are only first-order accurate [8].

B. Supercontinuum Generation

To examine the performance of the suggested RK4IP numerical scheme for simulations of broadband supercontinuum generation, a typical problem from the literature is now considered using the GNLSE (2). The exact fiber and laser parameters for this problem were taken from Dudley and Coen [19], and these parameters represent typical experimental conditions for supercontinuum generation in PCFs employing femtosecond lasers and pumping in the anomalous dispersion regime. The initial pulse that is used in the simulations has a hyperbolic secant

profile $A(0, T) = \sqrt{P_0}\mathrm{sech}(T/T_0)$, where the peak power P_0 is 10 kW, and the width T_0 is 28.4 fs, which corresponds to an intensity FWHM of 50 fs. The pulse is initially centered at 850 nm. The relevant fiber parameters, which represent a PCF or a tapered fiber, are shown in Table I. The soliton order for these conditions is around five. For the simulation of the supercontinuum, $N = 2^{13}$ time and frequency discretization points were employed.

The spectral evolution of the supercontinuum pulse at discrete locations along the fiber is shown in Fig. 2(a). Much more closely spaced spectra are also shown on a density plot in Fig. 2(b), where the spectral intensity is shown on a logarithmic density scale, which is truncated at -40 dB relative to the peak value. Dramatic spectral broadening is seen to already take place in the first centimeter of the fiber. This initial broadening, which is caused by the interaction between SPM and group-velocity dispersion, is symmetric. The spectrum quickly becomes asymmetric, and distinct spectral peaks develop on both sides of the pump wavelength as higher order dispersive and nonlinear perturbations cause the fission of the higher order soliton. The resulting fundamental solitons then undergo a continuous self-frequency shifting to longer wavelengths because of intrapulse Raman scattering. The emergence and self-shifting of one of these fundamental solitons on the long-wavelength side is clearly shown in Fig. 2(b). In this process, each Raman soliton sheds some of its energy in the form of a dispersive wave on the short-wavelength side of the pump, which also leads to the appearance of discrete spectral components in this region of the spectrum. The type of dynamics that is observed here is typical of supercontinua generated using ultrashort pulses in the anomalous dispersion regime of a highly nonlinear fiber [2], [6].

The numerical performance of the RK4IP scheme is now compared with the conventional schemes, in the same way as the case of the aforementioned second-order soliton. For the calculation of the average relative error ε at the end of the fiber ($z = 10$ cm), a reference supercontinuum trace that is calculated at the highest precision employed here (RK4IP method; $N_{\mathrm{steps}} = 316\,228$) was used for A^{true} in (13). It was verified that the use of reference supercontinuum traces that are calculated at the same precision using the slit-step Fourier schemes yielded the same result.

The results of this comparison are shown in Fig. 3, where the error ε, as a function of the number of computational steps
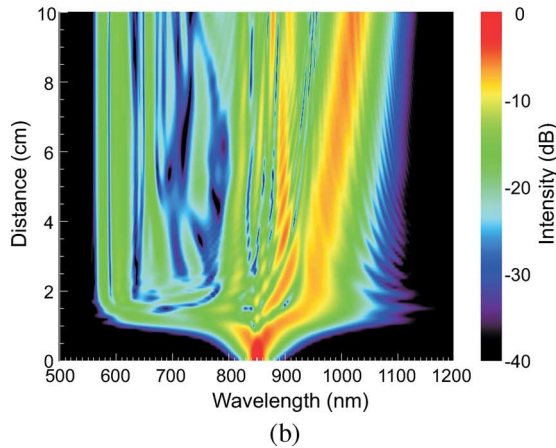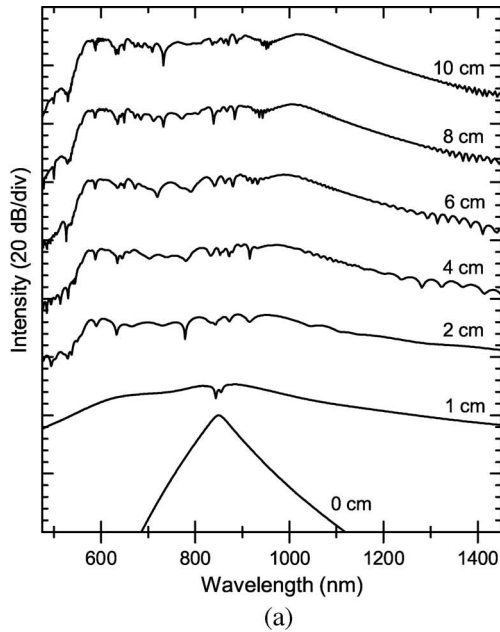
Fig. 2. Results from a numerical simulation of supercontinuum generation in a PCF. The spectral evolution as a function of the propagation distance is shown as (a) individual spectra and (b) intensity density plot.
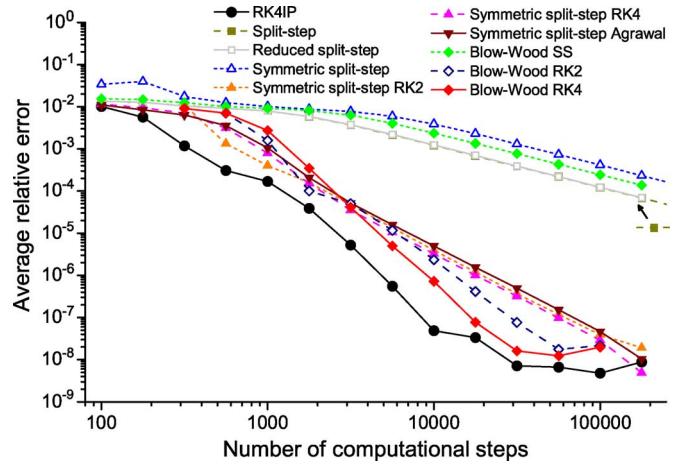

Fig. 3. Average relative error versus the number of computational steps for the generation of broadband supercontinuum radiation in a PCF.
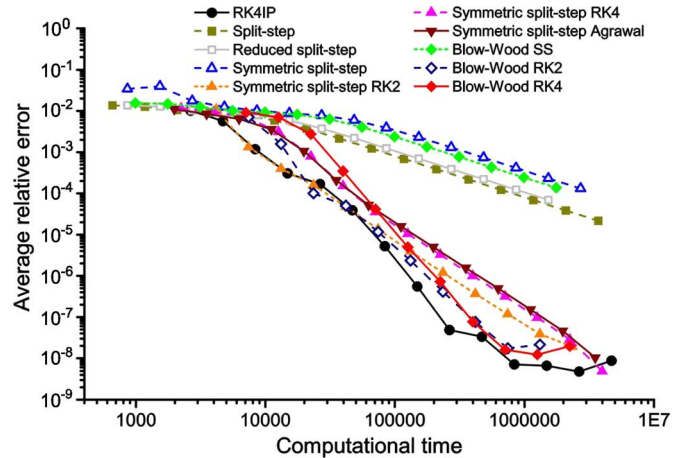

Fig. 4. Average relative error versus the computational time (normalized with the time required to calculate one FFT) for the generation of broadband supercontinuum radiation in a PCF.

N_{steps} employed, is plotted. The RK4IP method also exhibits the best performance for this more challenging problem and only requires about half the number of steps compared to the best of the competing schemes (Blow–Wood RK4). It exhibits the expected fourth-order accuracy over most of the span, with the numerical accuracy limit reached at $\varepsilon \approx 10^{-8}$. The Blow–Wood schemes again achieve first-, third-, and fourth-order accuracies for the Blow–Wood SS, Blow–Wood RK2, and Blow–Wood RK4 methods, respectively. Because of the poor accuracy at large step sizes, however, the overall difference in performance between the latter two is small. The symmetric split-step methods are all observed to be second-order accurate, except for the simplest symmetric split-step method, which is only first-order, and all yield very similar results. Thus, at the higher levels of precision required for supercontinuum simulations, they cannot compete with the RK4IP method. For the more complex nonlinearity that is currently encountered, the two simple split-step methods exhibit the expected first-order accuracy and yield inferior results.

As each tested method requires different numbers of FFTs and also different numbers of evaluations of the nonlinear operator per computational step, it is also of interest to consider the relative error as a function of computational effort, as is done in Fig. 4. Here, computational time has been normalized with the time required to evaluate one FFT. In the current implementation and for the present problem which was discretized into $N = 2^{13}$ gridpoints, each evaluation of the nonlinear operator (7) takes about five times longer than the time required to evaluate a single FFT. It should be noted that this ratio will vary with the number of employed gridpoints N.

The tolerated relative error strongly depends on the nature of the problem that is being studied. For the type of supercontinuum process that is simulated here, relative errors of 10^{-3} or smaller are required to numerically achieve stable results that are adequate for studying the physics of the process or for comparison with experimental results. In Fig. 4, the RK4IP algorithm offers the highest computational efficiency when the demands on accuracy are very high. However, even at the level of accuracy that is sufficient for studies of supercontinuum generation, the RK4IP method favorably compares with most of the other methods. It is as computationally efficient as the best

competing scheme (the symmetric split-step RK2 method) and is two to four times faster than most methods that are commonly employed for this purpose. The versatility of the RK4IP method is clear from the fact that it consistently exhibits good computational efficiency over a range of relative errors spanning almost six orders of magnitude, which makes it applicable to the study of a wide range of problems.

Finally, it is worth pointing out that, whereas fixed step sizes have been employed in all the simulations that are presented here, it is possible to implement an adaptive step-size selection with all the methods described in order to further minimize the computational effort [23]. The use of such adaptive step-size selection can also act to mitigate problems of spurious four-wave mixing, which are associated with the use of very large fixed step sizes [24], [25]. In the simulations presented here, such spurious four-wave mixing was observed in some cases, but its effect was negligible as the intensity of those four-wave mixing peaks was much weaker (typically < 50 dB) than the real spectral features.

IV. CONCLUSION

In this paper, an efficient method for the numerical solutions of the normal or general NLSEs that are used to describe pulse propagation in optical fibers is described. The RK4IP algorithm that is employed here was originally developed for numerical solutions of the time-dependent Gross–Pitaevskii equation, which is used to describe Bose–Einstein condensates. In this method, the problem is transformed into an interaction picture, which allows the use of conventional explicit techniques to put the solution forward. A highly efficient implementation is achieved by employing a fourth-order Runge–Kutta technique for stepping and by making an appropriate choice of separation between the normal and interaction pictures. The resulting method is easy to implement and exhibits a fourth-order global accuracy.

The performance of the RK4IP method was compared to a number of implementations of the split-step method by modeling both the propagation of a second-order soliton and the generation of supercontinuum radiation. The RK4IP method was observed to be globally fourth-order accurate for both problems studied. For the simulation of supercontinuum generation, it was also observed to be the most accurate of the methods tested.

REFERENCES

[1] *The Supercontinuum Laser Source*, 2nd ed. A. Alfano, Ed. New York: Springer-Verlag, 2006.

[2] J. M. Dudley, G. Genty, and S. Coen, "Supercontinuum generation in photonic crystal fiber," *Rev. Mod. Phys.*, vol. 78, no. 4, pp. 1135–1184, Oct./Dec. 2006.

[3] J. K. Ranka, R. S. Windeler, and A. J. Stentz, "Visible continuum generation in air–silica microstructure optical fibers with anomalous dispersion at 800 nm," *Opt. Lett.*, vol. 25, no. 1, pp. 25–27, Jan. 2000.

[4] T. A. Bartels, K. L. Corwin, N. R. Newbury, L. Hollberg, S. A. Diddams, J. W. Nicholson, and M. F. Yan, "420-MHz Cr:forsterite femtosecond ring laser and continuum generation in the 1–2-μm range," *Opt. Lett.*, vol. 28, no. 15, pp. 1368–1370, Aug. 2003.

[5] C. Lin and R. H. Stolen, "New nanosecond continuum for excited-state spectroscopy," *Appl. Phys. Lett.*, vol. 28, no. 4, pp. 216–218, Feb. 1976.

[6] G. P. Agrawal, *Nonlinear Fiber Optics*, 4th ed. San Diego, CA: Academic, 2007.

[7] J. W. Nicholson, A. K. Abeeluck, C. Headley, M. F. Yan, and C. G. Jørgensen, "Pulsed and continuous-wave supercontinuum generation in highly nonlinear dispersion-shifted fibers," *Appl. Phys. B, Photophys. Laser Chem.*, vol. 77, no. 2/3, pp. 211–218, Sep. 2003.

[8] T. Hohage and F. Schmidt, "On the numerical solution of nonlinear Schrödinger type equations in fiber optics," Konrad-Zuse-Zentrum für Informationstechnik, Berlin, Germany, Tech. Rep. ZIB-Report 02-04, Jan. 2002.

[9] W. H. Reeves, D. V. Skyabin, F. Biancalana, J. C. Knight, F. G. Omenetto, A. Efimov, and A. J. Taylor, "Transformation and control of ultra-short pulses in dispersion-engineered photonic crystal fibres," *Nature*, vol. 424, no. 6948, pp. 511–515, Jul. 2003.

[10] K. M. Hillingsøe, H. N. Paulsen, J. Thøgersen, S. R. Keiding, and J. J. Larsen, "Initial steps of supercontinuum generation in photonic crystal fibers," *J. Opt. Soc. Amer. B, Opt. Phys.*, vol. 20, no. 9, pp. 1887–1893, Sep. 2003.

[11] T. H. Z. Siederdissen, N. C. Nielsen, J. Kuhl, and H. Giessen, "Influence of near-resonant self-phase modulation on pulse propagation in semiconductors," *J. Opt. Soc. Amer. B, Opt. Phys.*, vol. 23, no. 7, pp. 1360–1370, Jul. 2006.

[12] K. J. Blow and D. Wood, "Theoretical description of transient stimulated Raman scattering in optical fibers," *IEEE J. Quantum Electron.*, vol. 25, no. 12, pp. 2665–2673, Dec. 1989.

[13] B. M. Caradoc-Davies, "Vortex dynamics in Bose–Einstein condensates," Ph.D. dissertation, Univ. Otago, Dunedin, New Zealand, 2000. [Online]. Available: http://www.physics.otago.ac.nz/bec2/bmcd/phdthesis/

[14] C. M. Savage, N. P. Robins, and J. J. Hope, "Bose–Einstein condensate collapse: A comparison between theory and experiment," *Phys. Rev. A, Gen. Phys.*, vol. 67, no. 1, p. 014 304, Jan. 2003.

[15] W. Wüster, J. J. Hope, and C. M. Savage, "Collapsing Bose–Einstein condensates beyond the Gross–Pitaevskii approximation," *Phys. Rev. A, Gen. Phys.*, vol. 71, no. 3, p. 033 604, Mar. 2005.

[16] R. G. Scott, C. W. Gardiner, and D. A. W. Hutchinson, "Nonequilibrium dynamics: Studies of the reflection of Bose–Einstein condensates," *Laser Phys.*, vol. 17, no. 4, pp. 527–532, Apr. 2007.

[17] V. E. Zakharov and A. B. Shabat, "Exact theory of two-dimensional self-focusing and one-dimensional self-modulation of waves in nonlinear media," *Sov. Phys.—JETP*, vol. 34, no. 1, pp. 62–69, 1972.

[18] Y. Kodoma and A. Hasegawa, "Nonlinear pulse propagation in a monomode dielectric guide," *IEEE J. Quantum Electron.*, vol. QE-23, no. 5, pp. 510–524, May 1987.

[19] J. M. Dudley and S. Coen, "Numerical simulations and coherence properties of supercontinuum generation in photonic crystal and tapered optical fibers," *IEEE J. Sel. Topics Quantum Electron.*, vol. 8, no. 3, pp. 651–659, May/Jun. 2002.

[20] R. H. Stolen, J. P. Gordon, W. J. Tomlinson, and H. A. Haus, "Raman response function of silica-core fibers," *J. Opt. Soc. Amer. B, Opt. Phys.*, vol. 6, no. 6, pp. 1159–1166, Jun. 1989.

[21] D. Hollenbeck and C. D. Cantrell, "Multiple-vibrational-mode model for fiber-optic Raman gain spectrum and response function," *J. Opt. Soc. Amer. B, Opt. Phys.*, vol. 19, no. 12, pp. 2886–2892, Dec. 2002.

[22] G. M. Muslu and H. A. Erbay, "Higher-order split-step Fourier schemes for the generalized nonlinear Schrödinger equation," *Math. Comput. Simul.*, vol. 67, no. 6, pp. 581–595, Jan. 2005.

[23] O. V. Sinkin, R. Holzlöhner, J. Zweck, and C. R. Menyuk, "Optimization of the split-step Fourier method in modeling optical-fiber communications systems," *J. Lightw. Technol.*, vol. 21, no. 1, pp. 61–68, Jan. 2003.

[24] F. Matera, A. Mecozzi, M. Romagnoli, and M. Settembre, "Sideband instability induced by periodic power variation in long-distance fiber links," *Opt. Lett.*, vol. 18, no. 18, pp. 1499–1501, Sep. 1993.

[25] G. Bosco, A. Carena, V. Curri, R. Gaudino, P. Poggiolini, and S. Benedetto, "Suppression of spurious tones induced by the split-step method in fiber systems simulation," *IEEE Photon. Technol. Lett.*, vol. 12, no. 5, pp. 489–491, May 2000.

Johan Hult received the M.Sc. and Ph.D. degrees in engineering physics from Lund University, Lund, Sweden, in 1998 and 2002, respectively.

He is currently an EPSRC Advanced Research Fellow with the Department of Chemical Engineering, University of Cambridge, Cambridge, U.K., where he joined as a Marie Curie Research Fellow in 2002. He is also the holder of a Senior Research Fellowship with Magdalene College, Cambridge. His research interests include atomic and molecular laser spectroscopy, reactive flow diagnostics, development of novel laser-based sensors, supercontinuum generation, and applications of supercontinuum light sources.